Study of Convergence Behavior of Real-Time Adaptive Active Noise Control Systems

Iman Tabatabaei Ardekani*, Waleed H. Abdulla
The University of Auckland, Private Bag 92019, Auckland, New Zealand
*Email: itab001@aucklanduni.ac.nz

***Abstract*—In adaptive active noise control systems, there is a theoretical upper-bound for the adaptation step-size beyond which the adaptation process of the control system becomes unstable. In practice, however, this upper bound is smaller than that suggested in theory. This is mainly because that theoretical analyses have been usually conducted for broadband white noise signals but in practice white noise signals are band-limited. This paper investigates the convergence behavior of a fully implemented real time adaptive active noise control system in an acoustic duct when the primary noise source produces different band-limited white noise. This investigation leads to an empirically-derived expression in closed-form for the upper-bound of the adaptation step size.**

I. Introduction

Active Noise Control (ANC) systems utilize an adaptive algorithm to update parameters, used in estimation of an anti-noise signal. This estimation should be made in such a way that the combination of noise and anti-noise signals, which are received at a desired silence zone, is minimized. It has been shown that traditional adaptive algorithms, e.g. Least Mean Square (LMS) algorithm, do not have acceptable behavior in ANC systems. [1], [2]. This is mainly because of existence of an electro-acoustic channel, which is called *secondary path*, in the path of the anti-noise signal to the silence zone. In order to solve this problem, *Filtered-x LMS* (FxLMS) algorithm has been proposed [3]. In this adaptive algorithm, the reference signal is filtered using an estimate of the secondary path before being used by the LMS algorithm. Similar to the LMS algorithm, the convergence rate of the FxLMS algorithm can be tuned up by adjusting an scalar parameter called *adaptation step-size* (μ). Increasing μ improves the convergence rate, but this parameter should be carefully increased because there is an upper-bound for this parameter (μ_{max}) beyond which the adaptation process becomes unstable.

There have been several contributions made in studying the effect(s) of the adaptation step-size on the stability or convergence of ANC systems. However, most of these studies were based on some simplifying assumptions regarding the secondary path and noise process, which are not applicable in practice. One major group of these studies relates to the case that the noise process is stochastic and can be modeled by a broadband white process. Elliott [4] showed that for a pure delay secondary path and broad-band white noise, μ_{max} is

$$\mu_{max} = \frac{2}{\sigma^2_{x_f}\,(L+\Delta)} \tag{1}$$

where $\sigma^2_{x_f}$ is the power of the filtered reference signal, L is the adaptive filter length and Δ is the overall delay in the secondary path. This result was derived based on simulation experiments and was not supported by any theoretical analysis. In [5], Long conducted a theoretical analysis for this simplified case and showed that

$$\mu_{max} = \frac{2}{\sigma^2_{x_f}\,(L+2\Delta)} \tag{2}$$

The same result was reported by Bjarnason in [6]. It has to be noted that values of μ_{max} which have been proposed by Elliott, Long and Bjarnason, were derived for the simplified case with the pure delay secondary path. In practice, such a simple secondary path does not exist. As a step forward estimation of a more reliable μ_{max}, the authors studied convergence of stochastic ANC systems with a more general secondary path, modeled by a moving average system [7]. They derived the following mathematical expression for μ_{max}.

$$\mu_{max} = \frac{2}{\sigma^2_{x_f}\,(L+2\Delta_{eq})} \tag{3}$$

where Δ_{eq} is called *Equivalent Delay of Secondary Path* and is calculated using parameters of the secondary path model $(s_0, s_1, \ldots, s_Q)$ as

$$\Delta_s = \frac{\sum_{q=0}^{Q} q s_q^2}{\sum_{q=0}^{Q} s_q^2} \tag{4}$$

This result have been found to be promising in simulation experiments, but practical experiments have shown that a realistic μ_{max} is smaller. This is because in practice the primary noise process is a band-limited white process, rather than a broadband white process. Even if the noise process is white over a wide frequency range, the reference signal (which provides the ANC system with primary noise information) is required to be filtered or conditioned with a sampling frequency higher than noise frequencies. Therefore, since a practical reference signal is always a band-limited signal, available convergence analyses cannot accurately model convergence behavior of ANC systems in practical conditions.

The aim of this paper is to practically investigate the effect(s) of the noise bandwidth on the convergence of FxLMS-based ANC systems by using a fully-implemented real-time ANC

Proceedings of the Second APSIPA Annual Summit and Conference, pages 534–537,
Biopolis, Singapore, 14-17 December 2010.

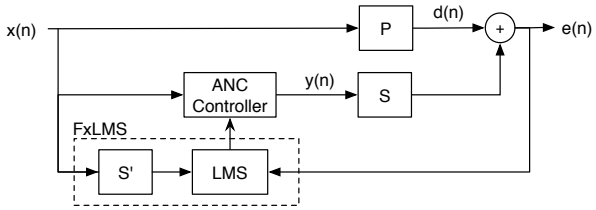

Figure 1. Block diagram of general active noise control system

system in an acoustic duct. This system has been designed and implemented using *National Instrument CompactRIO Control and Acquisition System* [8]. The main contribution of this paper is the derivation of the upper-bound for the adaptation step-size of FxLMS-based ANC systems in practical conditions. The rest of this paper is organized as follows. Next section describes presents FPGA design and implementation of a real-time adaptive ANC system in an acoustic duct. Section 3 represents results obtained from several experiments with the implemented system. Also, this section empirically derives a mathematical expression for the upper-bound of the adaptation step-size. Finally, Section 4 gives concluding remarks.

II. Real-Time Implementation of an Adaptive ANC System in An Acoustic Duct

The block diagram of an ANC system is shown in Figure 1. In this figure, $x\left(n\right)$ is the reference signal, $y\left(n\right)$ is the anti-noise signal which is generated by the ANC controller, $d\left(n\right)$ is the acoustic noise in the silence zone, and $e\left(n\right)$ is the residual noise signal. In practice, $x\left(n\right)$ is picked up by a microphone called *Reference Microphone,* $y\left(n\right)$ is played by a loudspeaker called *Canceling Loudspeaker* and $e\left(n\right)$ is measured by another microphone called *Error Microphone*. As shown in the figure, the acoustic noise $d\left(n\right)$ is assumed to be the response of the linear system P to the reference signal. Also, the secondary path which is the electro-acoustic channel from the output of the adaptive filter to the silence zone is modeled by a linear system S. In this figure $\acute{S}$ represents an available estimate of the secondary path S obtained by using on-line or off-line secondary path modeling techniques [9]. The ANC controller is an adaptive FIR filter of length L with weight vector

$$\mathbf{w} = \left[w_0, ..., w_{L-1}\right]^T \tag{5}$$

Therefore, the anti-noise which is the adaptive filter output is given by

$$y\left(n\right) = \mathbf{w}^T\left(n\right)\mathbf{x}\left(n\right), \tag{6}$$

$$\mathbf{x}\left(n\right) = \left[x\left(n\right), ..., x\left(n-L+1\right)\right]^T \tag{7}$$

where $\mathbf{x}\left(n\right)$ is the reference vector at time n and $\mathbf{w}\left(n\right)$ denotes the weight vector updated at time $n-1$. The FxLMS algorithm updates $\mathbf{w}\left(n\right)$ by using

$$\mathbf{w}\left(n+1\right) = \mathbf{w}\left(n\right) + \mu e\left(n\right)\mathbf{x}_f\left(n\right), \tag{8}$$

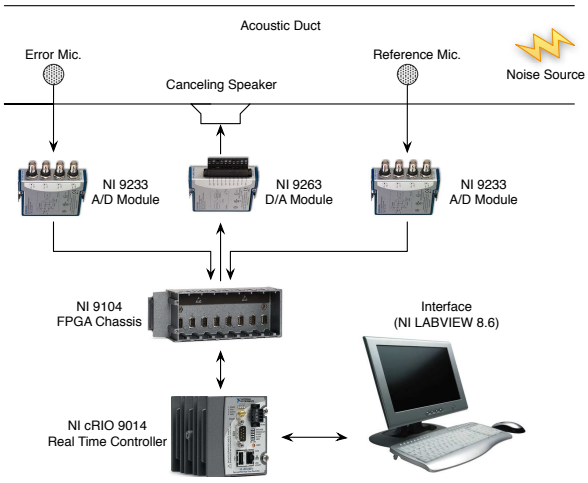

Figure 2. Schematic diagram of the implemented ANC system

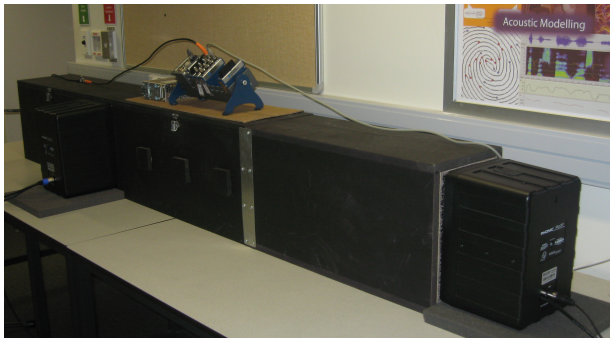

Figure 3. The implemented ANC system in the acoustic duct

where μ is the adaptation step-size, $e\left(n\right)$ is the residual noise signal picked up by the error microphone and $\mathbf{x}_f\left(n\right)$ is the filtered reference vector, obtained by passing $\mathbf{x}\left(n\right)$ through $\acute{S}$.

Figure 2 shows the schematic diagram of the implemented real-time adaptive ANC system in an acoustic duct and Figure 3 shows a photo of the actual system. The acoustic duct with dimensions of $1500cm \times 31cm \times 23cm$ was constructed from $1.8cm$ thick medium density fiber-board, with carpeted interiors. This duct was equipped with the following electr-acoustical components.

- NI 9104: Reconfigurable FPGA Chassis which utilizes an embedded Xilinx FPGA chip (clocked at 40MHz) to synthesize custom control and signal processing circuitry using LAB VIEW real-time development environment.
- NI CRIO-9014: a 400 MHz high performance real-time controller.
- NI 9233: a 24-Bit analog input module for CRIO embedded systems.
- NI 9263: a 16-Bit high-performance analog output modules for CRIO embedded systems.
- AKG-D770: 2 dynamic microphones with cardioid response pattern, used as the reference and error microphones. These microphones can be connected to NI9233

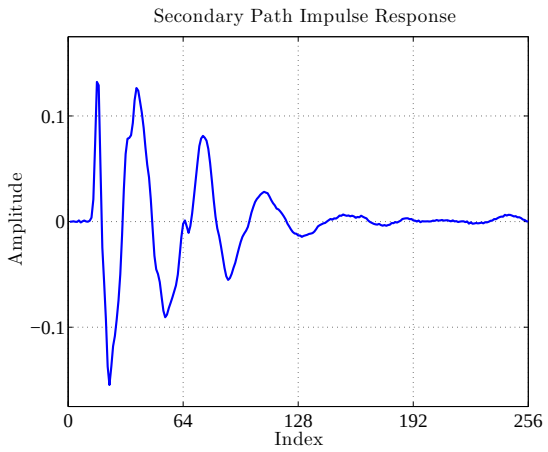

Figure 4. Impulse response of secondary path in experimental acoustic duct

input module using BNC connectors.

- Phonic SEp 207: a high performance loudspeaker with on-board 20W power amplifier, used as the canceling loudspeaker. This loud speaker can be also connected to NI9263 output module using another BNC connector.

The reconfigurable chassis, real-time controller, and I/O modules combine to create a complete stand-alone embedded system. The FPGA circuitry in the chassis controls each I/O module and passes data to the controllers through a local PCI bus using built-in communication functions. The FPGA design of the ANC system should be developed in *LAB VIEW FPGA Module* and compiled into a bit-stream file for download onto CRIO, where the design is synthesized in the FPGA chip. Our FPGA design has two parts; in the first part a real-time adaptive LMS algorithm for off-line modeling (identification) of the secondary path is implemented. In the second or main part a real-time adaptive FxLMS-based ANC system is implemented. The sampling frequency of the implemented system is $f_s = 6000Hz$, the length of the secondary path model is $Q = 256$ and the length of the adaptive filter vector is $L = 256$.

III. Results

In order to investigate convergence behavior of FxLMS-based ANC systems in practical conditions, this section conducts several examples using the implemented real-time ANC system. Figure 4 shows the secondary path impulse response of the acoustic duct which was estimated using the implemented real-time secondary path modeling system (off-line). Substituting coefficients of this impulse response into Eq. (4), the equivalent delay of this secondary path is computed as $\Delta_s = 38.32$.

We studied the convergence behavior of the implemented ANC system for 20 different band-limited primary noise and 3 different noise power levels. Therefore, 60 experiments has been conducted in total Different band-limited noise signals were generated using MATLAB and they were then stored in separate WAV files. These files can be played using a PC speaker, which is applied as the primary noise source. In each experiment, the step-size μ is incrementally changed and the minimum step-size that causes divergence is recorded in Table I as μ_{max}. In this table, the first column shows the normalized bandwidth of the primary noise (B_w) which is obtained by normalizing the band-width using sampling frequency ($f_s = 6000$). For example, $B_w = 0.2$ refers to the case that the primary noise is a band-limited white noise with bandwidth of $6000 \times 0.2 = 1200Hz$. Other columns show the empirically-obtained μ_{max} for 3 different noise power levels. Therefore, 3 different sets of data have been obtained. Now, in order to fit a reliable curve to the obtained results, we define variable x as

$$x \triangleq B_w \tag{9}$$

and variable y as

$$y \triangleq \frac{1}{\mu_{max}} \tag{10}$$

Now, we can plot data recorded in Table I in $x - y$ plane, as shown in Figure 5. We found out that the following curve can be fitted to the obtained empirical data.

$$y = \alpha + \frac{\beta}{x} \tag{11}$$

where α and β are two scalar parameters which can be computed using least square method [10]. Table II shows the

Table I
Experimental results

		$\sigma^2_{x_f} = 0.3$	$\sigma^2_{x_f} = 0.6$	$\sigma^2_{x_f} = 0.9$
#	B_w	μ_{max}	μ_{max}	μ_{max}
1	0.020	0.0010	0.0031	0.0020
2	0.050	0.0014	0.0038	0.0022
3	0.075	0.0017	0.0053	0.0027
4	0.100	0.0021	0.0059	0.0034
5	0.125	0.0029	0.0082	0.0040
6	0.150	0.0031	0.0085	0.0046
7	0.175	0.0037	0.0092	0.0045
8	0.200	0.0046	0.0098	0.0066
9	0.225	0.0035	0.0128	0.0055
10	0.250	0.0043	0.0119	0.0056
11	0.275	0.0041	0.0125	0.0060
12	0.300	0.0043	0.0148	0.0063
13	0.325	0.0046	0.0150	0.0069
14	0.350	0.0053	0.0129	0.0067
15	0.375	0.0054	0.0150	0.0070
16	0.400	0.0053	0.0146	0.0078
17	0.425	0.0059	0.0154	0.0081
18	0.450	0.0059	0.0170	0.0082
19	0.475	0.0047	0.0172	0.0095
20	0.500	0.0055	0.0159	0.0085

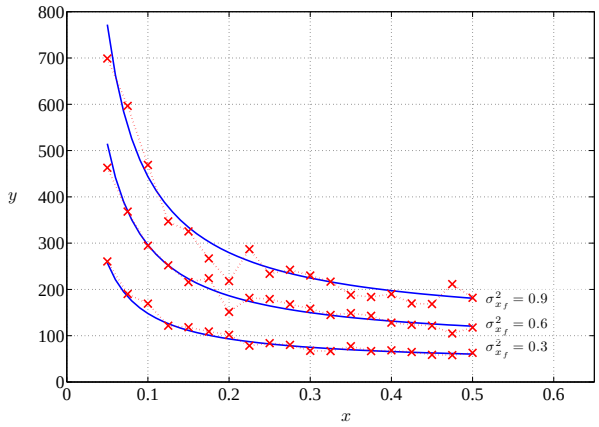

Figure 5. $y = \mu_{max}^{-1}$ versus $x = B_w$ for 60 different experiments with the implemented real-time ANC system (solid: fitted curve, dashed: Experimental results)

computed values of α and β for the 3 sets of data shown in Figure 5. For a general case, we suggest that

$$\alpha = 0.5\sigma^2_{x_f} L \tag{12}$$

and

$$\beta = \sigma^2_{x_f} \Delta_{eq} \tag{13}$$

Table II shows that values of α and β, which are computed using above equations, are approximately equal to those obtained using numerical least square method. The obtained curves for each set of data are plotted in Figure 5 using solid lines. As can be seen, there is a good agreement between empirical data and these curves. Now, combining Eqs. (9)-(13) results in

$$\frac{1}{\mu_{max}} = 0.5\sigma^2_{x_f} L + \frac{\sigma^2_{x_f} \Delta_{eq}}{B_w} \tag{14}$$

which leads to the following expression for μ_{max}.

$$\mu_{max} = \frac{2}{\sigma^2_{x_f} \left(L + \frac{2\Delta_{eq}}{B_w} \right)} \tag{15}$$

It can be easily seen that for a broadband white noise, where $B_w = 1$, Eqs. (3) and (15) are identical. In fact, this expression for μ_{max} is a generalization of Eq. (3) which has been previously proposed by the authors in [7]. It has to be noted that, in [7], Eq. (3) is derived using a theoretical analysis but this study proposes a more general equation using empirical results, which is applicable in practical conditions. Moreover, the agreement between the special case of the proposed result with $B_w = 1$ and that of [7] can be considered as the practical verification of theoretical results reported in [7].

IV. Conclusion

Previously derived upper-bound for the adaptation step-size of the FxLMS based ANC systems do not show enough reliability in practice. This is mainly because the available theoretical FxLMS convergence analyses have been usually carried out under the simplifying assumption that the primary noise is a broadband white signal. This paper, applied a fully implemented real-time ANC system in an acoustic duct in order to investigate convergence behavior of ANC systems in practical conditions. This empirical investigation leads to derive a mathematical expression for the upper-bound of the adaptation step-size in closed-form when the noise signal is assumed to be a band-limited white signal. In fact, the proposed expression can be considered as a generalization of the available theoretically-derived expression for the upper-bound of the adaptation step-size.

Table II
Numerical analysis of empirical data using least mean square method

	Least Square Method		Proposed Expression	
$\sigma^2_{x_f}$	α	β	$0.5\sigma^2_{x_f} L$	$\sigma^2_{x_f} \Delta_{eq}$
0.3	37.50	11.40	38.4	11.496
0.6	75.90	22.05	76.8	22.992
0.9	11.10	33.21	115.2	34.488

Acknowledgment

Authors would like to thank Mr. Matthew McCallum and Rhys Farrand for their contribution in the implementation of the ANC system, applied in this research.

References

[1] D. R. Morgan, "An analysis of multiple correlation cancellation loops with a filter in the auxiliary path," *Acoustics, Speech, and Signal Processing, IEEE International Conference on ICASSP '80.*, pp. 457–461, April 1980.

[2] J. C. Burgess, "Active adaptive sound control in a duct: computer simulation," *Journal of the Acoustical Society of America*, vol. 70, pp. 715–726, 1981.

[3] B. Widrow, D. Shur, and S. Shaffer, "On adaptive inverse control," in *Proceeding of the 15th Asilomar Conference on Circuits, Systems and Computers*, pp. 185–189, November 1981.

[4] S. J. Elliott and P. A. Nelson, "Multiple-point equalization in a room using adaptive digital filters," *Journal of the Audio Engineering Society*, vol. 37, pp. 899–907, November 1989.

[5] G. Long, F. Ling, and J. Proakis, "The lms algorithm with delayed coefficient adaptation," *IEEE Transactions on Acoustics, Speech and Signal Processing,*, vol. 37, pp. 1397–1405, Sep 1989.

[6] E. Bjarnason, "Analysis of the filtered-x LMS algorithm," *Speech and Audio Processing, IEEE Transactions on*, vol. 3, pp. 504–514, November 1995.

[7] I. Tabatabaei Ardekani and W. Abdulla, "Theoretical convergence analysis of FxLMS algorithm," *Signal Processing (2010), doi:10.1016/j.sigpro.2010.05.009*.

[8] National Instruments Corp., *CompactRIO-9012/9014 Operating Instructions and Specifications*, May 2008.

[9] S. M. Kuo and D. R. Morgan, *Active Noise Control Systems*. Wiley Interscience, 1996.

[10] O. Bretscher, *Linear Algebra With Applications*. Upper Saddle River NJ: Prentice Hall, 3rd ed. ed., 1995.